Interrogating the Effect of Bends on Two-Phase Gas-Liquid Flow using Advanced Instrumentation

Mukhtar Abdulkadir, Donglin Zhao, Safa Sharaf, Lokman Abdulkareem, Ian Lowndes and Barry Azzopardi

University of Nottingham, Faculty of Engineering, Process and Environmental Engineering Research Division, Institute
University Park, Nottingham, NG7 2RD, United Kingdom
ian.lowndes@nottingham.ac.uk

Keywords: bend, ECT, WMS, void fraction, flow regime

Abstract

When gas/ liquid mixtures flow around a bend they are subjected to forces additional to those encountered in a straight pipe. The behaviour of the flows at the inlet and outlet of the bend depends on the orientation of the pipes. Air/ silicone oil flows around a 90° bend have been investigated using advanced instrumentation: Electrical Capacitance Tomography (ECT), Hunt et al. (2004); Wire Mesh Sensor Tomography (WMS), Thiele et al. (2008); and high-speed video. The first two provide time and cross-sectionally resolved data on void fraction. The ECT probes were mounted 10 diameters upstream of the bend whilst the WMS was positioned either immediately upstream or immediately downstream of the bend. The downstream pipe was maintained horizontal whilst the upstream pipe was mounted either vertically or horizontally. The bend (R/D = 2.3) was made of transparent acrylic resin. From an analysis of the output from the tomography equipment, flow patterns were identified using both the reconstructed images as well as the characteristic signatures of Probability Density Function (PDF) plots of the time series of cross-sectionally averaged void fraction as suggested by Costigan and Whalley (1996). The superficial velocities of the air ranged from 0.047 to 4.727 m/ s and for the silicone oil 0.142 m/ s. Bubble/ spherical cap, slug, unstable slug and churn flows were observed before the bend for the vertical pipe and plug, slug, stratified flow when the pipe was horizontal. Bubble, stratified, slug and semi-annular flows are seen after the bend for the vertical 90 degree bend whilst for the horizontal 90 degree bend, the flow patterns remained the same as before the bend. These results are confirmed by the high-speed videos taken around the bend.

Gardner and Neller (1969) proposed a modified Froude number ($Fr_\theta = U_m^2 / Rg\sin\theta = 1$) criterion for the occurrence of stratification in a horizontal pipe downstream of a bend. However, the results obtained from the present study concluded that the downstream flow regime was stratified wavy flow.

Introduction

Production and transportation engineers in the onshore and offshore oil and gas industries have always been facing technical and environmental challenges associated with multiphase flows. For example, in an offshore environment, it is economically preferable to transport both gas and liquid through a single flow line and separate them onshore. In this way, a significant cost can be saved by eliminating the separate pipelines and phase separators at the offshore platform of Floating Production and Storage Operation. However, the instability problems caused by the multiphase flow can ultimately damage the pipeline system and this is unacceptable. The pipeline geometry contains not just straight pipes but also fittings such as, bends, valves, junctions and other fittings which make the flow gas and liquid more complicated. These fittings may lead to secondary flow, strongly fluctuating void fractions, flow excursions, flow separation, pressure pulsations and other unsteady flow phenomena. These phenomena can cause problems such as burn-out, corrosion, and tube failure, resulting in expensive outages, repairs, and early replacement affecting plant reliability and safety. Among these fittings, bends are often encountered in oil/gas production system because of: as a result of terrain undulation; flow line/riser combinations and at delivery points to production facilities. The presence of a bend can drastically change the flow patterns downstream of it. The flow redistribution phenomenon in bends, however, has received little attention. Literature on this subject is very limited. Most of the investigations have been restricted to single-phase flow (Eustice (1911); Dean (1927; 1928); Jayanti (1990); Dewhurst et al. (1990) and Spedding et al. (2004). A few papers, Gardner and Neller (1969), Carver (1984), Carver and Salcudean (1986), Ellul and Issa (1987), Legius and Akker (1997), Azzi et al. (2002), Azzi et al. (2005), Spedding et al. (2006), and Benbella et al. (2008), address the issue of gas-liquid systems but their experiments are confined to far smaller pipes than industry size and to the working fluids with physical properties very different from those dealt with by industry.

Single-phase flow in bends

Eustice (1911) published one of the earliest papers reporting flow in bends. He employed dye visualization studies with water. Laminar flow separation, reversal of flow and greater turbulence were observed in a 90º bend when $R/d<$ 3. His experiments demonstrated the existence of a transverse motion (secondary flow) superimposed on the primary flow, represented in the form of a pair of counter rotating longitudinal vortices.

Dean (1927; 1928) developed the first theoretical approach on the motion of a fluid in a curved pipe. This has been followed by several papers on this topic. Flow measurements using a 3-Dimensional LDA system in a square sectioned (0.1×0.1 m) 90 degree vertical bend was reported by Dewhurst et al. (1990). Streamwise and secondary velocities were obtained by these authors for water flow upstream of the bend and at 80º into the bend. Most of the studies of bends have been carried out for single phase flow. Jayanti (1990) reviewed the research into bends both under laminar and turbulent single phase conditions.

Gas-liquid flow in bends

Two-phase flow patterns observed in bends are qualitatively the same as those seen in straight pipes. However, bends introduce a developing situation in the flow pattern, whereby the relative positions and local velocities of the two phases are redistributed.

According to Spedding and Benard (2006) designers usually apply the general rule that a 90º elbow bend has a pressure drop equivalent of 30-50 pipe diameters length of straight pipe. However, a more exact method is desirable if the estimation of pressure drop can have a critical impact on operation or plant safety, such as on the downstream side of a relief valve.

Gardner and Neller (1969) carried out visual and experimental studies for bubble/ slug flow using a transparent pipe of 76 mm diameter in a vertical 90 degree bend of 305 and 610 mm radii of curvature, using air-water at atmospheric pressure. The local air concentrations over chosen cross-sections were measured. Their experimental date were used to interpret the effect of the competition between centrifugal and gravity forces on the flow distribution in bends. They found out that gas can either flow on the inside or outside of the bend depending on a critical Froude number defined as

$$Fr_\theta = \frac{U_m{}^2}{Rg\sin\theta} \tag{1}$$

where U_m, the mixture velocity, m/ s; R, the radius of curvature of the bend, m; θ, the angle of the bend. They claimed that if Fr_θ is greater than unity, the air will hug the inside of the bend, and if less than unity, the air will hug the outside of the bend. In the case of Fr_θ =1, both phases will be stratified. This conclusion, however, may not be valid for working liquids with different viscosity, density and surface tension.

Carver (1984) extended the work of Gardner and Neller (1969) using a 2-Dimensional (D) numerical computation method. They compared their results with those of Gardner and Neller (1969). The agreement was not particularly good. Carver and Salcudean (1986) recognized the limitations of using the 2-D numerical approach to simulate truly 3-D flows. They extended the 2-D model to 3-D and found that the 3-D model can give the similar trend as observed by Gardner and Neller (1969). Ellul and Issa (1987) developed an improved 3-D simulation where substantially different solution algorithm was adopted, a truncated gas momentum was added into their momentum equations and both air-water and gas-oil mixtures were considered. The simulation results showed better agreement with the experimental data than those obtained by the 2-D model in Carver (1984). No grid sensitivity analysis was reported in the work of Ellul and Issa (1987). The simulation result could not select the optimum mesh size. No experimental data was available at that time for them to validate their gas-oil simulation.

Legius and van der Akker (1997) carried out a numerical and experimental study in a bend of 630mm radius of curvature using air-water at atmospheric pressure. The experimental facility consisted of a transparent acrylic horizontal flowline (9 m long) connected to vertical riser (4m in height) by the 630 mm radius bend. The diameter of all pipes was 100 mm. Visual observation, 200 Hz digital camera and an Auto-regressive modelling method were used for flow regime identification. Slug and churn flow in the riser and stratified, slug and a new regime called "geometry enhanced slugging" in the flowline were identified. The time dependent behaviour of two-phase flow was modelled by an in-house code named Solution Package for Hyperbolic Functions (SOPHY-2). Good agreement between modelling and experiment results has been found under almost all conditions except at higher gas and lower liquid flow rates. However, the information presented for the characteristics of slug flow is limited. Important parameters like void fraction in liquid slug and Taylor bubble were not presented. The dependence of the Taylor bubbles and liquid slugs on the gas flow rates was not examined. The sample frequency of 50-100Hz used by these researchers seems too slow to get good spatial resolution of signals.

It can be concluded that most of the work reported in the literature on the multiphase flow in bends were carried out in small diameter pipes with air-water as the model fluids. Emphasis was on the determination of the pressure drop and phase distribution inside the bends. The change of flow structure before and after the bends was mainly obtained by visualization and the underlining mechanism for the change of flow patterns was not discussed. This paper is aimed to provide a more complete understanding on the flow phenomenon occurring in bends through the comprehensive experimental investigation in both vertical and horizontal pipes. The examined fluids are air and silicone oil, through which the effect of liquid viscosity and surface tension could be revealed. Advanced instruments such as Electrical Capacitance Tomography

(ECT), Wire Mesh Sensors (WMS) and high speed video camera have been used to measure void fractions before and after the bend. The flow patterns were determined by analyzing the Probability Density Function (PDF) of the time series of void fractions. This analysis was validated by the flow visualisation in the bend with the aid of a high speed video camera.

Nomenclature

d	pipe diameter (m)
D	Dimensional
Fr	Froude number (dimensionless)
g	gravitational constant (m/ s^2)
R	radius of curvature of the bend (m)
U	velocity (m/ s)
ε	cross-sectionally averaged void fraction

Subsripts

M	mixture
SG	superficial gas
SL	superficial liquid
θ	angle of bend

Experimental Facility

All experiments were carried out in an inclinable rig, shown in Figure 1, which had been employed earlier for annular flow studies by Azzopardi et al (1997), Geraci et al. (2007a), Geraci et al. (2007b) and latterly for bubbly, slug and churn flow studies by Hernandez Perez et al (2007), and Abdulkadir et al. (2010). The experimental facility consists of a main test section of the rig made from transparent acrylic resin pipes of 67 mm inside diameter and 6 m long to observe flow development over the test section. For all experiments, testing pipe were maintained at 6 m long from mixing section to make sure that they were long enough for flow development. The test pipe is set up so that it can be inclined from -5^o to 90^o being mounted on a rigid steel frame which could be positioned in intervals of 5^o, to enable the investigation of influence of different inclinations on flow regimes. In this paper only the experimental results obtained at the vertical and horizontal positions are discussed.

Air was supplied from laboratory compressed air main and measured by one of two variable area meters mounted in parallel. In addition, the static pressure of air was measured prior to entering the mixing section. Liquid was taken from a liquid storage tank and pumped by a centrifugal pump and metered by one of two variable area meters mounted in parallel. Air was mixed with liquid at the mixer before the mixture entered into the straight pipe, passed through a 90° bend and finally goes to a separator where air was released to the atmosphere from the top and liquid, under the influence of gravity, returned to main liquid storage. More details can be found in Abdulkadir et al. (2010)

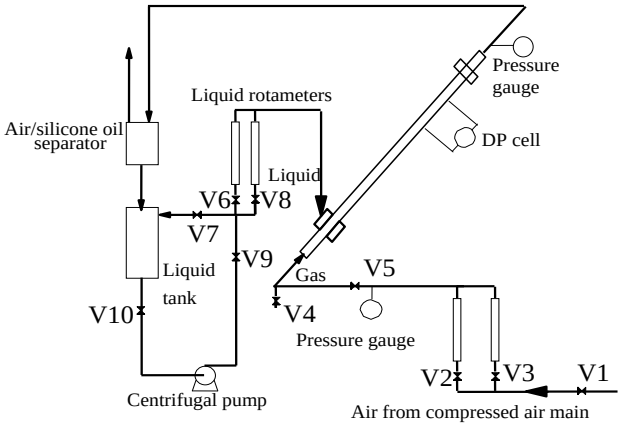

Figure 1: Schematic diagram of inclinable rig. This rig was converted to a vertical 90° bend and afterwards to horizontal 90° bend.

A 90° bend with a radius of curvature of 0.1544 m was mounted at the end of the straight pipe as shown in Figure 2. Downstream of the bend there is another straight pipe from which the gas-liquid mixture enters a flexible pipe that takes it to the phase separator. Two bend positions were investigated: (1) vertical bend with upstream, vertical riser and downstream horizontal flowline and (2) horizontal bend with horizontal flow lines upstream and downstream. The behaviour of the air-silicone oil mixture was examined using the ECT and WMS.

A detailed description of the theory behind the ECT technology is described by Hammer (1983), Huang (1995), Zhu et al. (2003) and Azzopardi et al. (2008). The method can image the dielectric components in the pipe flow phases by measuring rapidly and continually the capacitances of the passing flow across several pairs of electrodes mounted uniformly around an imaging section. Thus, the sequential variation of the spatial distribution of the dielectric constants that represent the different flow phases may be determined. In this study, a ring of electrodes were placed around the circumference of the riser at a given height above the injection portals at the bottom of the 6 m riser section. This enabled the measurement of the instantaneous distribution of the flow phases over the cross-section of the pipe.

The WMS technology, described in detail by Da Silva et al. (2010) can image the dielectric components in the pipe flow phases by measuring rapidly and continually the capacitances of the passing flow across several crossing points in the mesh. It consists of two planes of 24 stainless steel wires with 0.12 mm diameter, 2.78 mm wire separation within each plane and 2 mm axial plane distance. This determined the spatio/ temporal resolution of the sensor. Since the square sensor is installed in a circular tube, only 440 of the total 576 wire crossing points are within the radius of the tube (Abdulkadir et al. (2010)). During the experiments, the horizontal transmitter lines are pulsed one after another. By measuring the signal of all crossing vertical receiver wires, the local capacitance around the crossing points in the mesh is known. This capacitance signal is a measure for the amount of silicone

oil, and thus indicates the local phase composition in the grid cell.

The ECT was placed 4.49 m (67 diameters) away from the mixing section while the WMS was placed at about 4.92 m (73 diameters) away from the mixing section. The WMS was afterwards located at a distance of about 0.021m (3 diameters) after the bend. The experiments were performed at room temperatures (15-20 degree Celsius). The properties of the two fluids used in the experiments are as shown in Table 1. The influence of the bend orientation on the flow behaviour was studied by changing the position of the bend from vertical to horizontal.

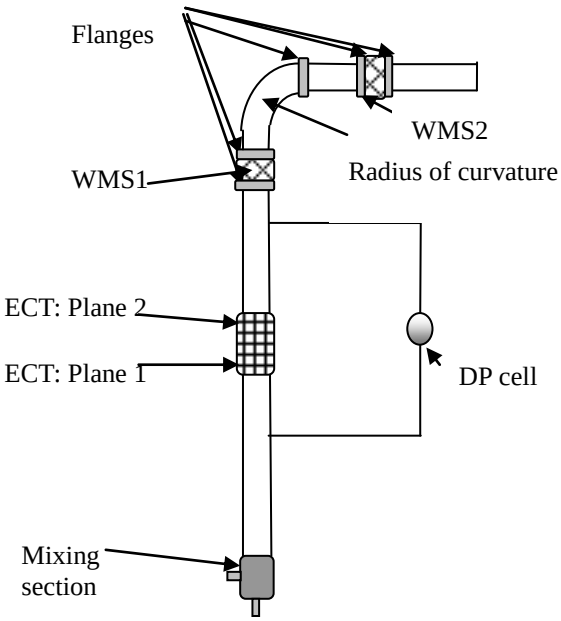

Probes	distance from mixing section
ECT plane 1	4.40 m
ECT plane 2	4.489 m
WMS1	4.92 m
Radius of Curvature	0.1544 m

Figure 2: Schematic diagram of vertical 90 degree bend present study. The downstream pipe was maintained horizontal whilst the upstream pipe was mounted vertically or horizontally. This rig was instrumental to take physical measurements that could be used to characterize the flow regime existing before and after the bend when the flow rates of both the oil and the air injection were varied

Table 1: Properties of the fluids

Fluid	Density (kg/ m^3)	Viscosity (kg/ ms)	Surface tension (N/ m)
Air	1.18	0.000018	
Silicone oil	900	0.00525	0.02

Results and Discussion

Several runs were carried out with air-silicone oil mixture mainly for the purpose of defining and classifying all the two-phase flow patterns attainable with the experimental rig using the ECT and WMS. The liquid superficial velocity investigated was 0.142 m/ s and gas superficial velocities ranged from 0.047 to 4.727 m/ s. In each of these runs, independent visual observations and flow characteristics were recorded in detail for the vertical riser, bends, and flowline (horizontal pipe). To test the accuracy of the ECT and WMS, a comparison was made based on bends, and flowline (horizontal pipe). To test the accuracy of the ECT and WMS, a comparison was made based on the Probability Density Function (PDF) of void fraction. The results of the PDF of void fraction were further reinforced by the cross-sectional slice view of void fraction obtained from the WMS. Comparisons between the flow regimes before and after the bends were made based on the PDF of void fraction. All the flow regimes for the vertical and horizontal 90º bends were then categorized based on the basis of visual observations and supported by high speed video image. It was observed that the transition from one flow regime to another was gradual with respect to fluid flow rates.

Comparison of PDFs of void fraction for the ECT and WMS for the riser before the bend and reconstructed images of the two-phase flow as depicted by the WMS

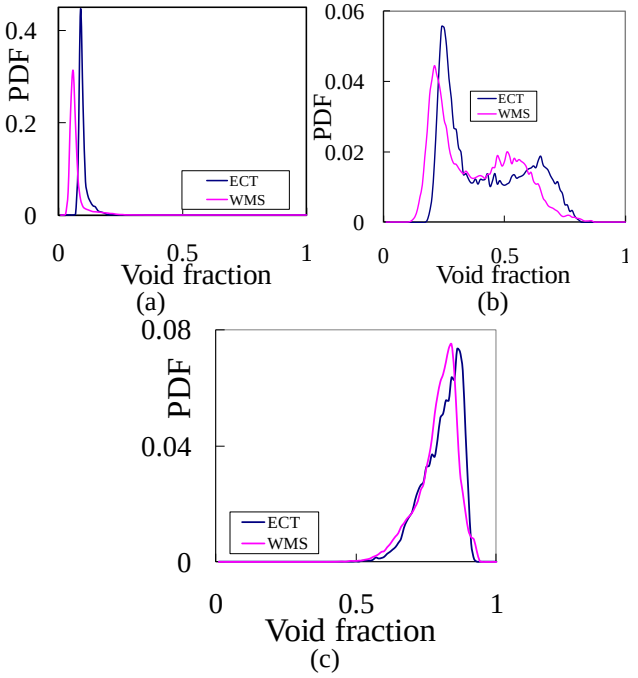

Figure 3: Comparison of PDFs of void fraction for the ECT and WMS before the bend. In all cases the liquid superficial velocity was 0.142 m/ s. Gas superficial velocities: (a) 0.047m/ s (b) 0.544 m/ s (c) 4.727 m/ s.

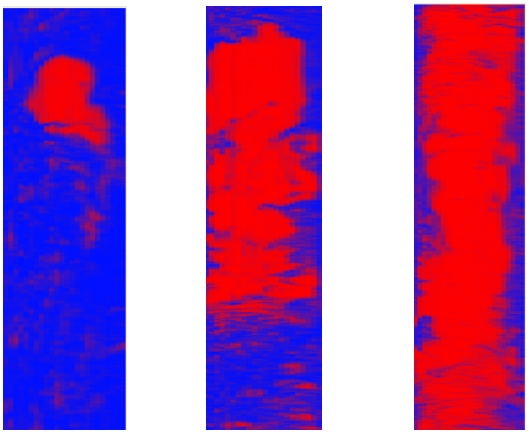

(a) **(b)** **(c)**

Figure 4: Reconstructed images of the two-phase flow transition from spherical cap bubble to churn flow. In all cases the liquid superficial velocity was 0.142 m/ s. Gas superficial velocities: (a) 0.047m/ s (b) 0.544 m/ s (c) 4.727 m/ s.

Figures 3a to 3c presents the comparison between the PDFs of void fraction for the ECT and WMS for same flow conditions in a vertical riser. The plots show that at a liquid superficial velocity of 0.047 m/ s and a gas superficial velocity of 0.047 m/ s, both the ECT and WMS defined the flow regime as spherical cap bubble.
However, the ECT provides a higher PDF while the WMS predicts higher void fraction. Increasing the gas superficial velocity to 0.544 m/ s whilst maintaining same liquid velocity of 0.142 m/ s the characteristic signature of the flow regime according to both the ECT and WMS is slug flow. It can also be observed that the ECT still provide higher PDF of void fraction than the WMS but with a lesser range compared to at gas superficial velocity of 0.047 m/ s while the WMS provide a higher void fraction. At a gas superficial velocity of 4.727 m/ s, the ECT and WMS both defined the flow pattern as churn flow. It is interesting to note that both the PDF of void fraction for ECT and WMS show almost same peak. The degree of agreement of the length of the PDF and void fraction improves with an increase in gas superficial velocity. The result therefore shows that both instruments predict the same signature. Figures 8a to 8c show 2D slice view for the void fractions observed for different gas superficial velocities to support the result obtained in Figure 3a to 3c. At a gas superficial velocity of 0.047 m/ s, there are still bubbles of large size, but not as big as the pipe diameter. When the gas velocity is increased to 0.544 m/ s, coalescence starts leading to slug flow. At gas superficial velocity of 4.727 m/ s, the slug flow transforms into churn flow. This results obtained are in agreement with the results obtained in Figures 3a to 3c.

Comparison of PDFs of void fraction before and after the bend using the WMS

Table 2: PDF of void fraction before and after the bend

Flow conditions	PDF of void fraction before the bend	PDF of void fraction after the bend
Liquid superficial velocity = 0.142 m/ s Gas superficial velocity = 0.047 m/ s	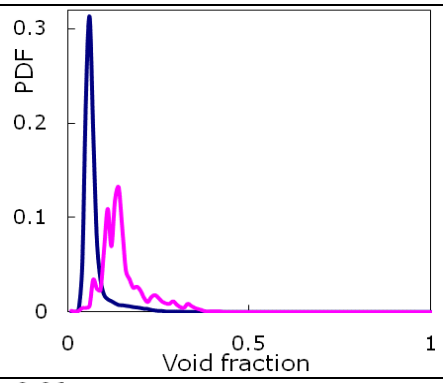	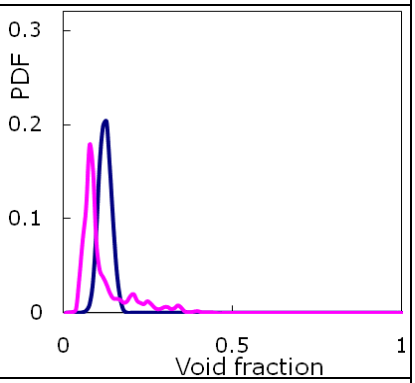
Liquid superficial velocity = 0.142 m/ s Gas superficial velocity = 0.544 m/ s	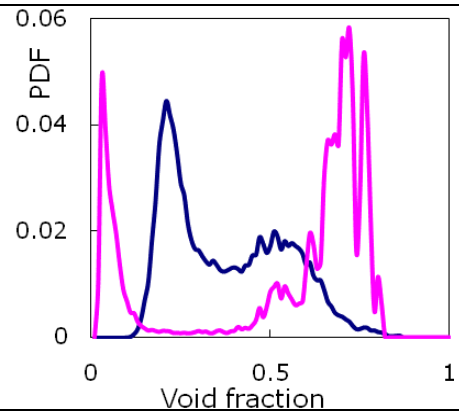	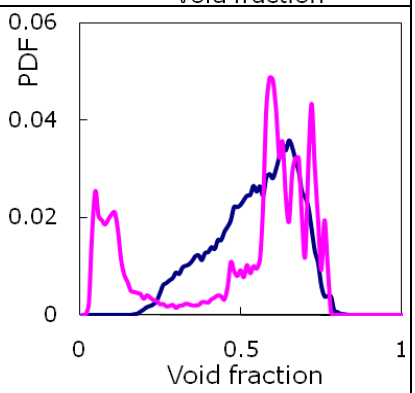

Liquid superficial velocity = 0.142 m/ s Gas superficial velocity = 0.945 m/ s	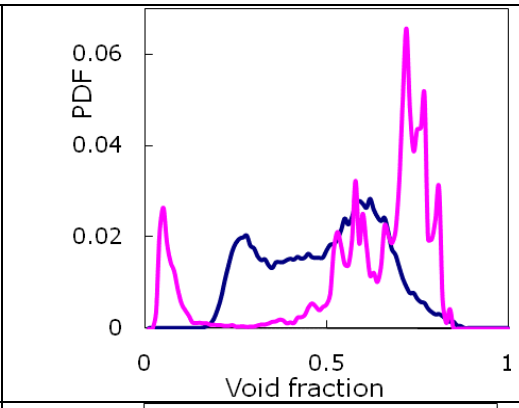	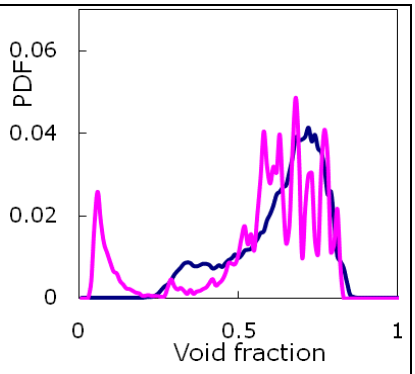
Liquid superficial velocity = 0.142 m/ s Gas superficial velocity = 2.363 m/ s	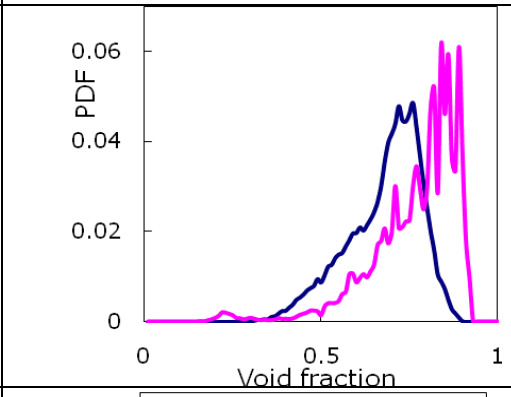	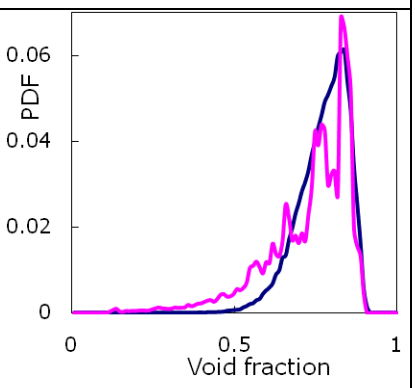
Liquid superficial velocity = 0.142 m/ s Gas superficial velocity = 4.727 m/ s	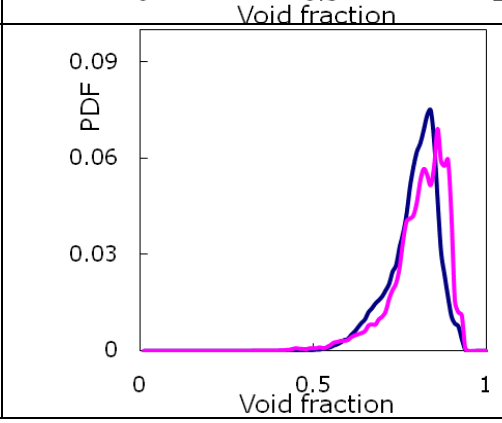	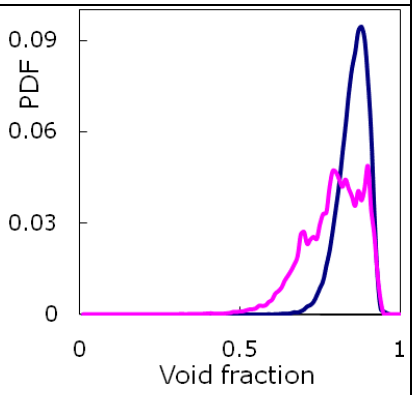

PDF is the rate of change of the probability that void fraction values lie within a certain range ($0 \le \varepsilon \le 1$) versus void fraction. The PDF of time varying void fractions has been used to classify the flow patterns in the same manner as Costigan and Whalley (1996) and Omebere-Iyari and Azzopardi (2007). A single peak at low void fraction represents bubble flow and a double peak feature with one at low void fraction whiles the other one at high void fraction represents slug flow. A single peak at low void fraction accompanied by a broadening tail represents spherical cap bubble whiles a single peak at a high void fraction with a broadening tail represents churn flow.

The PDFs of the void fraction data obtained at a fixed liquid superficial velocity 0.142 m/ s and variable gas superficial velocities ranging from 0.047 to 4.727 m/ s are shown in Table 2. The flow conditions are given in the first column of the Table 2. In the second column, the PDF for the riser before the vertical bend (the blue curve) are compared with that for the flowline before the horizontal bend (the red curve) at the same flow conditions. The third column gives the same comparison for the scenario after the bend.

At the low gas flow rate (gas superficial velocity = 0.047 m/ s), the PDF for the vertical riser presents a single peak of the void fraction value at about 0.06 with a broadening tail extending to a higher value of about 0.35. This defines a "Spherical cap bubble flow" as in Costigan and Whalley (1996). The flow pattern has been confirmed by the images of high speed video camera as shown in Figure 5. The gas bubbles indeed exhibit spherical cap shapes. When the vertical riser was positioned to become horizontal (flowline), the PDF of the void fraction at the same flow rate, shows a dominant peak at 0.14 with a wide base spanning from 0 to 0.36. This is the typical feature of plug flow. The elongated gas bubbles are separated by sections of continuous liquid moving downstream along the top part of the pipe with almost zero void fractions in the liquid. The variation of the void fraction reflects the different size of the gas bubbles and the continuous liquid phase. After

the bend, the PDF for the horizontal pipe in the riser shows a single peak, the signature of bubbly flow. The broaden tail present in the PDF of the riser does not exist in the PDF after the bend. The big cap bubbles break up in the bend due to the balance of the centrifugal force and the surface tension. The bubbles become more uniform. For the horizontal setup, the PDF after the bend move to the lower void fraction values with the dominant peak frequency at the void fraction of 0.08. There is little change in the size of the wide base compared with that before the bend. With the same mechanism the elongated bubbles break in to smaller bubbles when passing through the bend. The flow patterns are still kept as plug flow though.

When the gas flow rate increases to 0.544 m/ s, the cap bubbles coalescence into bullet-shaped Taylor bubbles and the slug flow are formed. The PDF of the void fractions in the riser gives two main peaks at the values of 0.2 and 0.5 respectively. These peaks are the signature of the aerated liquid slugs and the Taylor bubbles with the different sizes. Taylor bubbles have yet fully developed. This claim is confirmed by the analysis of the video images as shown in Figure 6. Similar to that for the riser, the PDF for the horizontal flowline has one narrow peak at the value of 0.02 and one wide peak with fluctuations at around 0.7. With the increase of gas superficial velocity from 0.047 to 0.544 m/ s, the elongated bubbles grow and coalescence into bullet-shaped Taylor bubbles. The flow pattern changes from the plug flow to the slug flow. After the bend, the PDF of the void fraction in the flowline for the riser has a "hill" shape. Stratified wavy flow was observed. For the horizontal setup, compared with the PDF before the bend, the lower void fraction peak moves to the higher void fraction values and more peaks appear at the void fractions 0.5 - 0.8. This can probably be attributed to the collapse of the big Taylor bubbles while passing through the bend. However, the flow pattern remained as slug flow.

When the gas flow rate reaches 0.945 m/ s, again two peaks appear on the PDF graph of void fractions for the riser but the height of the lower void fraction peak decreases more than 50% while the probability density of the higher void fraction increases more than 40% compared with those at 0.544 m/ s. The increase of gas superficial velocity leads to the increase of Taylor bubbles and the shrinkage of the liquid slugs. More and more bubbles are entrained in the liquid slugs. This regime according to Costigan and Whalley (1996) is defined as unstable slug flow. For the case of the flowline arrangement, the height of the lower void fraction peak also decreases significantly. The PDF curve moves to the higher void fraction values with the increase of the gas superficial velocity. After the bend for the riser setup, with the increase of U_{SG} from 0.544 to 0.945 m/ s, the stratified wavy flow in the flowline becomes the developing slug flow, which is featured by a small peak superimposed on a big peak with a wide base. With the increase of U_{SG} from 0.544 m/ s the waves becomes stronger and as consequence more bubbles are trapped inside. At a certain point the Taylor bubbles are formed. For the horizontal setup, no significant difference is present in the PDF between before and after the bend except the significant reduction in the height of the peak at the high void fraction (~0.72).

At 2.363 m/ s, the PDF of void fraction for the riser has a single peak at about 0.76 with broadened tails down to 0.2 and 0.9. This is the typical feature of churn flow. An increase of the gas superficial velocity escalates the instability of liquid slugs. When the speed of gas core reaches to a certain point, the liquid slugs will be penetrated and the integrity of the Taylor bubbles will be destroyed. This leads to the transition to churn flow. For the horizontal setup, released liquid from the collapsed slugs accumulates on the bottom part of the pipe and strong wave caused by the gas travel on the upper part of the pipe. Stratified wavy flow is formed. After the bend, the PDF of the void fractions for the riser significantly shifts to the higher values compared with that before the bend. The dominant void fraction from 0.75 increases to 0.83 and its count increases more than 40%. The churn flow before the bend changes to stratified wavy after the bend. This has been confirmed by visualization analysis. The liquid film, however, is erratic and showed large disturbances with void fractions down to about 0.7. For the horizontal arrangement, no significant flow pattern change was observed. It keeps the same stratified wavy after the bend.

At the highest gas flow rate of 4.727 m/ s we examined, the PDF of void fractions for the riser has very similar shape to that at 2.363 m/ s but with much narrower tails. The peak moves towards the higher void fraction. The flow pattern is still the churn flow, but close to the transition to the semi-annular flow. For the horizontal layout, with the increase of gas flow rate from 2.363 to 4.727 m/ s, the liquid film becomes more and more uniformly distributed around pipe wall. This is reflected on the PDF curve where the peak becomes narrower and exhibits less fluctuation. The annular flow regime is approached when the gas superficial velocity is big enough to distribute evenly the liquid on the pipe wall. After the bend, semi-annular flow is present in the flowline for the riser and stratified wavy appears in the flowline for the horizontal arrangements.

Flow patterns using high speed video images

A. Flow regimes in vertical riser (vertical 90 degree bend)

Given below are descriptions of the various flow regimes in the other that they might be expected to occur for constant liquid flow rate and increasing air flow rate:

Spherical cap bubble: here as shown in Figure 5, there is an increase in bubble coalescence and agglomeration. The bubbles are now forming larger ones, but not big enough to cover the pipe diameter. The velocity of a bubble may differ substantially from that of the liquid phase.

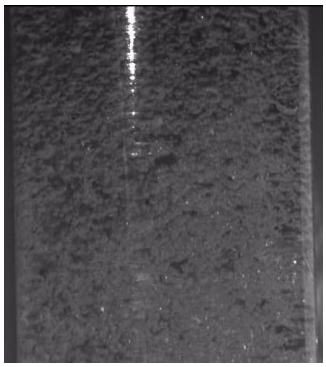

Figure 5: Video image of spherical cap bubble for a riser at liquid superficial velocity = 0.142 m/ s and gas superficial velocity = 0.047 m/ s.

Slug flow: the gas is observed to flow as large bullet shaped bubbles separated by large silicone oil droplets with some gas entrained in it. Figure 6 show that part of the liquid from the Taylor bubble travel downwards as a film on the pipe axis as thin lines.

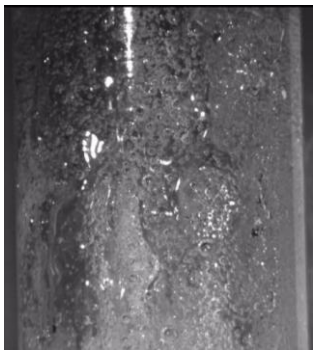

Figure 6: Video image of slug flow for a riser at liquid superficial velocity = 0.142 m/ s and gas superficial velocity = 0.544 m/ s.

Unstable slug: the flow pattern shown in Figure 7 obtained at higher gas flow rates represents the transition to churn flow. An increase in gas coalescence in the liquid slug as a consequence of an increase in gas flow rate brought about oscillating of the liquid slug, thereby causing the liquid slug to begin to collapse.

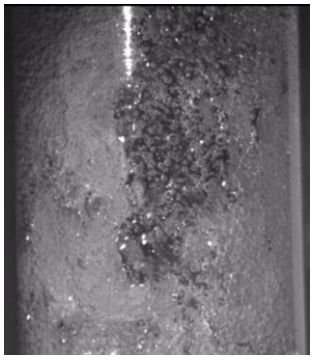

Figure 7: Video image of unstable slug flow at liquid superficial velocity = 0.142 m/ s and gas superficial velocity = 0.945 m/ s.

Churn flow: as the gas flow rate increases further as shown in Figure 8, the unstable slug flow regime seizes to exist as a result of breakdown of all of the liquid slugs. The breakdown slugs are now distributed in the form of waves on an annular film.

Figure 8: Video image of churn flow for a riser at liquid superficial velocity = 0.142 m/ s and gas superficial velocity = 2.363 m/ s.

B. Flow regimes in bend (vertical 90 degree bend)

The two dominant factors governing the flow structure of a two-phase flow mixture in the 90 degree bends were the flow regime as the mixture entered the bends and the interaction of gravitational and centrifugal forces.

Spherical cap bubble: the flow regime of the mixture entering the bend is spherical cap bubble with the size of the bubbles almost occupying the entire cross-section of the pipe. On entering the bend, the bubbles migrate to and follow the inside of the bend while the liquid to the outside of the bend. The liquid on striking the wall creates secondary flow. When the secondary flow meets with the primary (incoming) flow, bigger bubbles are created as a consequence of high level of mixing. The created bubbles as a result of low surface tension forces collapse almost immediately. The gravity forces then takes the liquid to the inside of the bend while the gas to the outside of the bend as shown in Figure 9.

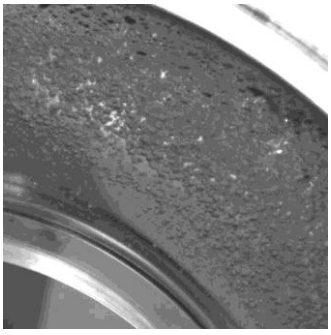

Figure 9: Video image of spherical cap bubble flow passing through a vertical 90 degree bend at liquid superficial velocity = 0.142 m/ s and gas superficial velocity = 0.047 m/ s.

Slug and unstable flows: the centrifugal force takes the Taylor bubble to the inside of the bend whilst the liquid to the outside of the bend. The gravitational force then takes the liquid to the inside of the bend while the Taylor

bubbles to the outside of it as shown in Figure 10a. The interesting thing that happened here is that as the Taylor bubble is moving up due to buoyancy and the liquid downwards due to gravity forces, at equilibrium, the Taylor bubble collapsed completely as depicted in Figure 10b. The collapsed bubble created a dry patch occupying almost 100% of the bend. This region which is shown in Figures 10c and 10d is wetted periodically but can endure for a reasonably long period of time. The bubble collapse could be due to gravity forces overcoming the low surface tension force of silicone oil. Liquid moving with high momentum on the other hand, move in forward direction while the ones with the lesser momentum moves backward.

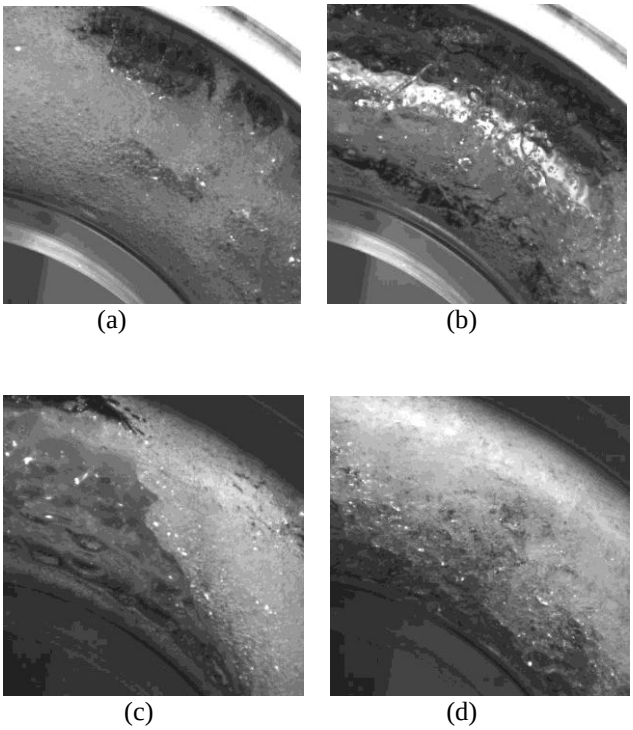

(a) (b)

(c) (d)

Figure 10: Video image of stable slug flow passing through a vertical 90 degree bend at liquid superficial velocity = 0.142 m/ s and gas superficial velocity = 0.047 m/ s.

Churn flow: the same mechanism could be taking place for both the slug and churn flows. However, not all of the bubbles collapsed, the bigger bubbles remained at the centre of the bend while the smaller ones spread in all directions as shown in Figure 11a. Also, there was no dry patch observed in this regime. Some of the bigger bubbles are sent inside the bend by the centrifugal forces. As the bubbles strike the bottom of the bend due centrifugal forces, they collapse and drain downwards. This is reflected in Figure 11b

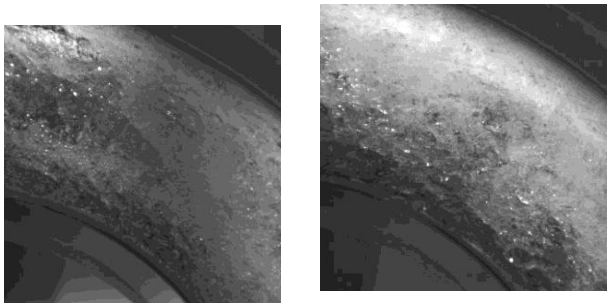

(a) (b)

Figure 11: Video image of churn flow passing through a vertical 90 degree bend at liquid superficial velocity = 0.142 m/ s and gas superficial velocity = 0.047 m/ s.

C. Flow regimes in flowline (horizontal 90 degree bend)

For flowline (horizontal) up flow, a different form of classification had to be established; because gravity introduces an asymmetry into the flow: the density difference between both phases causes the liquid to travel preferentially along the bottom of the pipe. These flow regimes are described below also in order of increasing gas flow rate.

Plug flow: gravity effect cause the gas plugs to move along the top of the pipe. The level of liquid in the pipe is full to almost the diameter of the pipe.

Slug flow: this regime is characterized by the intermittent appearance of slugs of liquid which bridge the entire pipe section and move at almost the gas velocity. Lots of pressure fluctuations typify this flow regime observed at much higher gas flow rates; where the gas pressure behind the slugs is greater than in front of the slug. The length of the Taylor bubble decreases with an increase in gas flow rate whilst maintaining a constant liquid flow rate.

Stratified wavy flow: at higher gas velocities, the shearing action of the gas at the interface generates large amplitude waves on the liquid surface. Liquid is torn from the surface of these waves giving rise to droplet entrainment in the gas core. The deposition of these drops partially wet the top of the pipe.

D. Flow regimes in bend (horizontal 90 degree bend)

Plug flow: the gas plugs on entering the bend initially migrate towards the inner radius of the bend under the influence of centrifugal force, but subsequently it is forced outward due to the increasing influence of gravity.

Slug flow: at higher gas flow rate, the centrifugal force moves the liquid to the outside of the bend while the gas to the inside of the bend. The gravity force then takes the liquid to the inside of the bend and the gas to the outside of the bend. The Taylor bubble then collapsed almost immediately, leaving behind dry patches in the bend. This same behaviour was observed for the slug flow in the vertical 90º bend.

Stratified wavy flow: the level of liquid in the pipe has dropped to less half the diameter of the pipe with an increase in gas flow rate leading to collapse of the Taylor bubble.

Competition between centrifugal and gravitational forces

This section will aim to study the effect of bend on flow separation. It will be based on a modified Froude number proposed by Gardner and Neller (1969) that when Fr = 1, there will be stratified flow after the bend. Also that when Fr is greater than 1, air will move to the inside of the bend, whilst when Fr is less than 1, air will move to the outside of the bend.

Table 3: Comparison between present work and the works of Gardner and Neller (1969) based on modified Froude number.

Work	Before the bend	Fr_θ	After the bend
Gardner and Neller (1969)	Bubbly/ slug flow	1.00	Stratified flow
Present work	Bubbly flow	0.997	Stratified wavy flow

It can be observed from Table 3 that the value of Fr from the present study is 0.997 (≈ 1). The flow regime before and after the bend are bubbly and stratified wavy flows respectively whilst for Gardner and Neller, bubbly and stratified flows are observed before and after the bend respectively. This discrepancy may be due to the fact that the viscosity of silicone oil is about 5 times that of water and with a surface tension about 2/ 7 times that of water.

Conclusions

Interrogating the effect of bends on two-phase gas-liquid flow has been successfully investigated using advanced instrumentation, ECT and WMS. The WMS has 24 X 24 steel wires with 0.12 mm diameter and measures the cross-sectional void fractions at 440 locations. The data were taken at an acquisition frequency of 200 and 1000 Hz for the ECT and WMS respectively over an interval of 60 seconds. The characteristic signatures of Probability Density Function derived from the time series of cross-sectionally averaged void fraction data were used to identify the flow patterns. The results were validated by the analysis of the recorded high speed video images. The examined ranges of U_{SG} and U_{SL} are 0.047 to 4.727 m/ s and 0.142 to 0.378 m/ s respectively. We have found that:

1) The ECT and WMS predicted same flow pattern signatures.
2) With an increase of U_{SG} from 0.047 to 4.727 m/ s, spherical cap bubble, slug, unstable slug and churn flows were observed in the vertical riser while in the horizontal flowline, plug, slug and stratified wavy flows were developed. Certainly buoyancy force plays an important role in the formation of the different flow patterns.
3) Bends have significant effect on the gas-liquid flow. In both the vertical and horizontal 90 degree bends gravitational force tends to move the liquid to the inside of the bend while the gas to the outside of the bend. Some big spherical cap bubble and Taylor bubbles break up in the bends due to the balance of the centrifugal force and the surface tension. The bubbles become more uniform. Dryness patch in the bend was observed in the slug and unstable slug flows. As a result, after the vertical bend the spherical cap bubble flow became bubbly flow, and the churn flow turn to stratified wavy and semi-annular flows. The horizontal bend has less effect on the flow patterns compared with the vertical bend.
4) Gardner and Neller (1969) proposed a modified Froude number ($Fr_\theta = U_m^2 / Rg\sin\theta = 1$) condition for stratified flow after the bend. However, the result obtained in the present study proved otherwise. The result obtained was stratified wavy. This result is to be expected in view of the fact that the viscosity of silicone oil is about 5 times that of water and with a surface tension about 2/ 7 times that of water.

Acknowledgements

M. Abdulkadir would like to express sincere appreciation to the Nigerian government through the Petroleum Technology Development Fund (PTDF) for providing the funding for his doctoral studies.

Donglin Zhao and Safa Sharaf are funded by EPSRC under grant EP/ F016050/ 1.

This work has been undertaken within the Joint Project on Transient Multiphase Flows and Flow Assurance. The Author(s) wish to acknowledge the contributions made to this project by the UK Engineering and Physical Sciences Research Council (EPSRC) and the following: - GL Industrial Services; BP Exploration; CD-adapco; Chevron; ConocoPhillips; ENI; ExxonMobil; FEESA; IFP; Institutt for Energiteknikk; PDVSA (INTEVEP); Petrobras; PETRONAS; SPT; Shell; SINTEF; Statoil and TOTAL. The Author(s) wish to express their sincere gratitude for this support.

References

Abdulkadir, M., Hernandez-Perez, V., Sharaf, S., Lowndes, I. S. & Azzopardi, B. J., Phase distributions of an air-silicone oil mixture in a vertical riser, HEFAT 2010, 7th International Conference on Heat Transfer, Fluid Mechanics and Thermodynamics, Antalya, Turkey 2010.

Azzi, A. & Friedel, L. Two-Phase Upward Flow 90 Degree Bend Pressure Loss Model, Forschung im Ingenieurwasen Vol. 69, 120- 130 2005.

Azzi, A., Friedel, L., Kibboua, R. & Shannak, B. Reproductive Accuracy of Two-Phase Flow Pressure Loss Correlations for Vertical 90 Degree Bends, Forschung im Ingenieurwasen Vol. 67, 109- 116 2002.

Azzopardi, B. J. Drops in annular two-phase flow, Int. J. Multiphase Flow, Vol. 23, S1-S53. 1997.

Azzopardi, B. J., Hernandez Perez, V., Kaji, R., Da Silva, M. J., Beyer, M. & Hampel, U. Wire mesh sensor studies in a vertical pipe, HEAT 2008, Fifth International Conference on Multiphase Systems, Bialystok, Poland. 2008.

Azzopardi, B.J., Jackson, K., Robinson, J.P., Kaji, R., Byars, M. & Hunt, A. Fluctuations in dense phase pneumatic conveying of pulverised coal measured using electrical capacitance tomography. Chem. Eng. Sci., Vol. 63, 2548-2558 (2008).

Benbella, S., Al-Shannag, M. & Al-Anber, Z. A. Gas-liquid pressure drop in vertically wavy 90 degree bend. Experimental Thermal and Fluid Science 2008.

Carver, M.B., Numerical computation of phase separation in two fluid flow, ASME Paper No. 82-FE-2, Vol. 106/ 153 1984.

Carver, M.B, & Salcudean, M., Three-dimensional numerical modelling of phase distribution of two- fluid flow in elbows and return bends, Numerical Heat Transfer, Vol. 10, 229-251 (1986).

Costigan, G. & Whalley, P.B. Slug flow regime identification from dynamic void fraction measurements in vertical air-water flows, Int. J. Multiphase Flow, Vol. 23, 263-282 (1996).

Da Silva, M.J., Thiele, S., Abdulkareem, L., Azzopardi, B.J. & Hampel, U. High-resolution gas-oil two-phase flow visualization with a capacitance wire-mesh sensor.. Flow Measurement and Instrumentation, (2010Accepted

Dean, W.R. Note on the motion of a fluid in a curved pipe. Phil. Mag., Vol. 4, 208-223(1927).

Dean, W.R. Stream- line motion of a fluid in a curved pipe. Phil. Mag., Vol. 5, 673-695 (1928).

Dewhurst, S. J., Martin, S.R., Jayanti, S., & Costigan, G., Flow measurements using 3-D LDA system in a square section 90 degree bend, Report AEA-In Tech-0078 (1990).

Ellul, I.R., & Issa, R.I. Prediction of the flow of interspersed gas and liquid phases through pipe bends. Trans. Instn. Chem. Engrs, Vol. 65, 84-96 (1987).

Eustice, J. Flow of water in curved pipes. Proc. R. Soc., A84, 107-118 (1910).

Gardner, G..C. & Neller, P.H. Phase distributions flow of an air-water mixture round bends and past obstructions, Proc. Inst. Mech. Engr., Vol. 184, 93 -101 (1969).

Geraci, G., Azzopardi, B.J. & Van Maanen, H.R.E. Inclination effects on circumferential film distribution in annular gas/ liquid flows. AIChE Journal, Vol. 53. 1144-1150 (2007a).

Geraci, G., Azzopardi, B.J. & Van Maanen, H.R.E. Effects of inclination on circumferential film thickness variation in annular gas/ liquid flows. Chem. Eng. Sci., Vol. 62, 3032-3042 (2007b).

Hammer, E.A. Three-component flow measurement in oil/ gas/ water mixtures using capacitance transducers, PhD thesis, University of Manchester (1983).

Hernandez-Perez, V. Gas-liquid two-phase flow in inclined pipes. PhD Thesis, University of Nottingham, United Kingdom (2007).

Huang, S.M.. Impedance sensors-dielectric systems. In R. A. Williams, and M. S. Beck (Eds.), Process Tomography, Cornwall: Butterworth-Heinemann Ltd. (1995).

Jayanti, S. Contribution to the study of non-axisymmetric flows. PhD Thesis, Imperial College London (1990).

Legius, H.J.W.M. & van den Akker, H.E.A. Numerical and experimental analysis of translational gas-liquid pipe flow through a vertical bend. Proceedings of the 8th International Conference, BHR Group, Cannes, France (1997).

Manera, A., Ozar, B., Paranjape, S., Ishii, M. & Prasser, H.–M. Comparison between wire-mesh-sensors and conducting needle-probes for measurements of two-phase flow parameters. Nucl. Eng. Des. Vol. 239, 1718-1724 (2008).

Omebere-Iyari, N.K. & Azzopardi, B.J. A study of flow patterns for gas/ liquid flow in small diameter tubes. Chem. Eng. Res. Design, Vol. 85, 180-192 (2007).

Spedding, P.L. & Benard, E. Gas-liquid two-phase flow through a vertical 90 degree elbow bend, Exp. Thermal Fluid Sci., Vol. 31, 761-769 (2006).

Spedding, P.L. & Benard, E. & McNally, G.M.. Fluid Flow through 90 Degree Bends, Dev. Chem. Eng. Min. Process Vol. 12, 107-128 (2004).

Thiele, S., Da Silva, M.J., Hampel, U., Abdulkareem, L. & Azzopardi, B.J. High-resolution oil-gas two-phase flow measurement with a new capacitance wire-mesh tomography. 5th International Symposium on Process Tomography in Poland, Zakopane, 25-26 August (2008).

Zhu, K., Madhusudana Rao, S., Wang, C. & Sundaresan, S. Electrical capacitance tomography measurements on vertical and inclined pneumatic conveying of granular solids. Chem. Eng. Sci. Vol. 58, 4225-4245 (2003).